

Nylon-6 Nanocomposites from Alkylammonium-Modified Clay: The Role of Alkyl Tails on Exfoliation

T. D. Fornes,[†] D. L. Hunter,[‡] and D. R. Paul^{*,†}

Department of Chemical Engineering and Texas Materials Institute, The University of Texas at Austin, Austin, Texas 78712, and Southern Clay Products, 1212 Church Street, Gonzales, Texas 78629

Received November 3, 2003

ABSTRACT: Nylon-6–organoclay nanocomposites were prepared by melt processing via twin-screw extrusion for the purpose of comparing the effect of the number alkyl groups attached to the nitrogen of the organic modifier on the level of organoclay exfoliation. Wide-angle X-ray scattering and transmission electron microscopy techniques were employed to assess the morphology developed in each type of nanocomposite, while stress–strain diagrams were used to evaluate mechanical property performance. Nanocomposites derived from an organoclay having no alkyl tails in the quaternary cation result in an immiscible morphology, consisting primarily of unexfoliated clay particles, whereas those derived from an organoclay having one alkyl tail in the quaternary cation lead to a well-exfoliated morphology. Increasing the number of alkyl tails to two produced a mixed structure comprised of a large fraction of clay stacks intercalated with polymer as well as a fraction of dispersed clay platelets. The extent of mechanical reinforcement parallels the degree of exfoliation. Overall, the results may be explained by the competition between the effects of platelet–platelet interactions and the interaction of the polymer with the organoclay platelet.

Introduction

The formation of well-exfoliated polymer–clay nanocomposites is dependent upon a variety of factors, one being the structure of the organic compound used to modify the clay.^{1–7} Prior work in this laboratory¹ on the effect of the structure of the alkylammonium compound on the level of exfoliation achieved in nylon-6 during melt processing revealed that the most pronounced changes in nanocomposite morphology, as well as mechanical properties, result from altering the number of long alkyl groups or tails attached to the nitrogen of the modifier. Specifically, organic modifiers consisting of one long alkyl tail lead to significantly higher levels of organoclay exfoliation than those having two alkyl groups. This result is believed to stem from the amount of silicate surface that the alkylammonium cation allows to be exposed to the polyamide. It appears that nylon-6, owing to its polarity or strong hydrogen-bonding ability, has some affinity for the pristine surface of the clay, certainly more so than for the largely aliphatic organic modifier. It was proposed that the organic modifier consisting of two alkyl tails shields more silicate surface than one alkyl tail and, thus, precludes desirable interactions between the polyamide and the clay surface, which ultimately limits the degree of organoclay exfoliation. A logical question arises from this proposal: will organic modifiers containing no long alkyl tails lead to even better exfoliation in nylon-6? The aim of this paper is to address this question by comparing morphological and mechanical property data for melt-processed nylon-6 nanocomposites based on organoclays whose organic cations possess zero, one, and two long alkyl tails.

Experimental Section

Materials and Melt Processing. Table 1 lists the materials used in this study.⁸ The organoclays shown were formed by the exchange of various quaternary ammonium ions (see Figure 1) and the sodium ions of native montmorillonite (cation exchange capacity (CEC) = 92 mequiv/100 g of clay); the level of amine added was near stoichiometric proportion, i.e., 95 mequiv/100 g of clay, to that of the CEC of the sodium montmorillonite. A simple nomenclature system is used to designate the structure of the amine cation in the organoclay (see Figure 1); the symbols M and HT represent methyl and hydrogenated tallow, respectively. Tallow is a natural product consisting of a distribution of saturated and unsaturated hydrocarbon chains with a majority of chains (~63%) 18 carbons in length.^{8,9} Nanocomposites were formed by extruding each organoclay with a high molecular weight grade of nylon-6 (HMW) using a Haake corotating twin-screw extruder set at a barrel temperature of 240 °C, a screw speed of 280 rpm, and a feed rate of 980 g/h, as previously described.^{1,10,11} The exact amount of montmorillonite (MMT) in each nanocomposite was determined by placing predried extruded pellets in a furnace at 900 °C for 45 min and weighing the residual ash. The resulting value was corrected for loss of structural montmorillonite that occurred during the incineration.^{12,13} The weight percentage of MMT in the final nanocomposite was calculated from

$$\% \text{ MMT} = \% \text{ MMT}_{\text{ash}}/0.935 \quad (1)$$

where % MMT_{ash} is the mass after incineration relative to the original nanocomposite mass.

If one wishes to know the actual weight percentage of organoclay within the nanocomposite, this can be determined by the following relation:

$$\% \text{ organoclay} = \% \text{ MMT}_{\text{ash}} \left[\frac{\text{LOI}}{1 - \text{LOI}} - 0.0695 \right] + \% \text{ MMT} \quad (2)$$

where LOI represents the mass loss on ignition per gram of dry organoclay when heating pure organoclay at 900 °C for

[†] The University of Texas at Austin.

[‡] Southern Clay Products.

* Corresponding author: Tel 512-471-5392; fax 512-471-0542; e-mail drp@che.utexas.edu.

Table 1. Materials Used in This Study

material [designation used here]	commercial designation (source)	comments/specifications
nylon-6 [HMW]	Polymer Capron B135WP (Honeywell)	high viscosity extrusion grade, $\bar{M}_n = 30\,100^a$
tetramethyl montmorillonite [M ₄] ^b	Organoclays experimental	95 MER, ^c % LOI = 14.9 wt %, ^d d_{001} spacing = 1.36 nm
trimethyl hydrogenated-tallow ammonium montmorillonite [M ₃ (HT) ₁] ^b	experimental	95 MER, ^c % LOI = 29.6 wt %, ^d d_{001} spacing = 1.80 nm
dimethylbis(hydrogenated-tallow) ammonium montmorillonite [M ₂ (HT) ₂] ^b	Cloisite 20A (Southern Clay Products)	95 MER, ^c % LOI = 39.6 wt %, ^d d_{001} spacing = 2.42 nm

^a \bar{M}_n , in units of daltons, was determined via intrinsic viscosity using *m*-cresol at 24.6 °C.⁸ ^b The substituents on the quaternary ammonium compound used to form the organoclay are identified in this shorthand notation where M = methyl and HT = hydrogenated tallow. Tallow is a natural product composed predominantly (~63%) saturated and unsaturated hydrocarbon chains 18 carbons in length. HT is the saturated form yet still contains a small fraction of double bonds. ^c MER stands for milliequivalent ratio and represents the level of amine added during the in exchange reaction with sodium montmorillonite; i.e., 95 MER corresponds to 95 mequiv of amine added per 100 g of sodium montmorillonite. ^d The loss on ignition (LOI) is the amount of volatiles evolved from per gram of dry organoclay when heating it to 900 °C for 45 min.

Structure	Designation	No. of Alkyl Tails
	M ₄	0
	M ₃ (HT) ₁	1
	M ₂ (HT) ₂	2

Figure 1. Molecular structures used to organically modify sodium montmorillonite by ion exchange. The symbols M and HT designate methyl and hydrogenated tallow groups attached to the nitrogen.

45 min. Note that the first set of terms on the right side of eq 2 corresponds to the weight percent organic modifier within the nanocomposite, while the latter term, % MMT, corresponds to the weight percent inorganic as defined in eq 1. Equation 2 can be simplified into the following form by substituting eq 1 into eq 2:

$$\% \text{ organoclay} = \frac{\% \text{ MMT}_{\text{ash}}}{1 - \text{LOI}} \quad (3)$$

Extruded nanocomposite pellets were injection molded into standard tensile (ASTM D638) and Izod bars (ASTM D256) using an Arburg Allrounder 305-210-700 injection molding machine set at a barrel temperature of 260 °C, an injection pressure of 70 bar, a holding pressure of 35 bar, and a mold temperature of 80 °C. All polyamide-containing materials were dried under vacuum at 80 °C for minimum of 16 h prior to any melt processing step.

Characterization. The morphology of the nanocomposites was examined using wide-angle X-ray scattering (WAXS) and transmission electron microscopy (TEM). WAXS scans were performed on injection-molded Izod bars, as well as on organoclay powder, in the reflection mode at a scan rate of 1°/min using a Scintag XDS 2000 diffractometer using Ni filtered Cu K α X-ray radiation ($\lambda = 0.154$ nm). Samples for TEM analysis were extracted from compression-molded films obtained by pressing ~10 g of dried nanocomposite pellets in a Wabash

compression-molding machine at 10 kpsi and 230 °C. Ultrathin sections, approximately 70–90 nm in thickness, were examined by TEM using one of two Phillips/EM microscopes (EM 208 and 301 series) both operating at an accelerating voltage of 80 kV.

The mechanical behavior of the nanocomposites was characterized via tensile tests according to ASTM D638 using an Instron model 1137 testing frame. Modulus and yield strength were measured at a crosshead speed of 0.51 cm/min, while elongation at break was determined at 0.51 and 5.1 cm/min using a gauge length of 9.08 cm. An extensometer was used to accurately determine Young's modulus. Tensile property values reported here represent an average of six samples; standard deviations were typically on the order of 4% for modulus, 1% for yield strength, and between 5 and 25% for elongation at break.

Results

Figure 2 shows the effects of the number of alkyl tails on the ammonium cation on the X-ray scattering behavior of the organoclays M₄, M₃(HT)₁, and M₂(HT)₂ and their corresponding nanocomposites based on high molecular weight (HMW) nylon-6. Increasing the size of the ammonium cation by replacing methyl groups with alkyl groups results in increased organoclay *d* spacings (lower 2θ values). In other words, the gallery of montmorillonite expands to accommodate more mass of organic material for the fixed level of exchange capacity. Extruding each organoclay with a HMW nylon-6 leads to substantially different WAXS patterns for the three types of nanocomposites. The X-ray pattern for the nanocomposite derived from the M₄ organoclay shown in Figure 2a is virtually identical to its organoclay X-ray pattern, suggesting that nylon-6 chains failed to intercalate the organoclay during melt processing, thereby resulting in immiscible structures or clay tactoids. The presence of one alkyl tail in the organic modifier, however, leads to a smooth, nanocomposite X-ray pattern (see Figure 2b), indicating breakup or delamination of the once ordered organoclay. The X-ray scan for the nanocomposite based on the two-tail modifier, M₂(HT)₂, is suggestive of an intercalated morphology, since strong reflections are observed at *d* spacings higher than those of the pure organoclay (see Figure 2c). Note that increasing the basal spacing of the organoclay does not necessarily lead to more exfoliation.

The TEM photomicrographs shown in Figure 3 provide visible evidence of the conclusions from the WAXS data. The nanocomposite derived from the M₄ organoclay having no alkyl tails contains predominantly un-

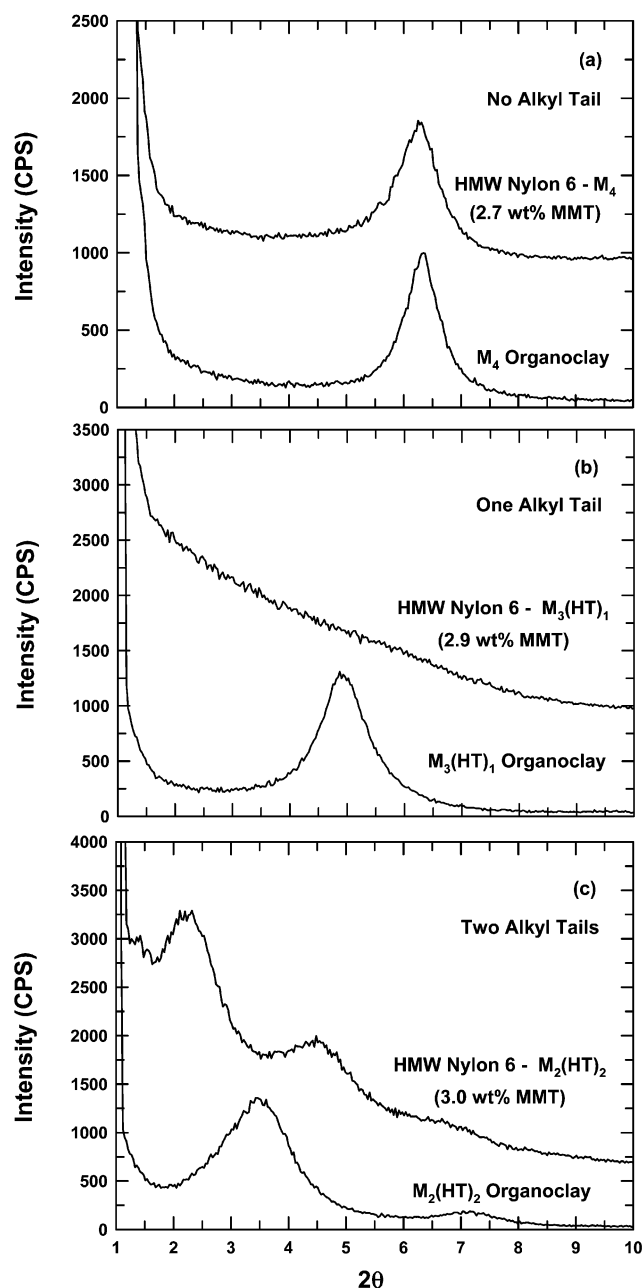


Figure 2. WAXS scans of the organoclay and corresponding nanocomposites based on HMW nylon-6 for quaternary ammonium cations having (a) zero, (b) one, and (c) two alkyl tails.

exfoliated clay tactoids distributed throughout the polymer (see Figure 3a), whereas the nanocomposite based on the one tail organoclay, $M_3(HT)_1$, exhibits a well-exfoliated morphology consisting primarily of individually dispersed clay platelets (see Figure 3b). The nanocomposite based on the two-tail organoclay, $M_2(HT)_2$, is comprised of a large fraction of unexfoliated clay particles in addition to individually dispersed platelets. Also evident in the photomicrographs of three nanocomposites is the inverse relationship between the level of exfoliation and the distance between clay particles for a given clay concentration. For example, the nanocomposite derived from the M_4 organoclay, which consists of an unexfoliated morphology and the least amount of exfoliation, exhibits the largest distances between clay particles (see Figure 3a), whereas the opposite is true for the well-exfoliated nanocomposite based on $M_3(HT)_1$ (see Figure 3b).

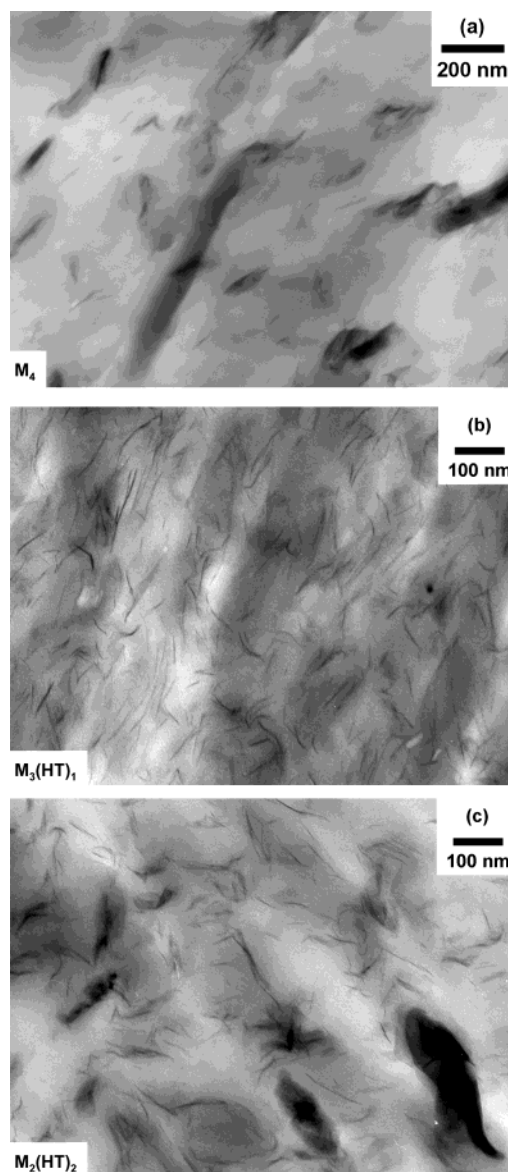


Figure 3. TEM photomicrographs of HMW nylon-6 composites based on the organoclays (a) M_4 , (b) $M_3(HT)_1$, and (c) $M_2(HT)_2$ containing 2.7, 2.9, and 3.0 wt % MMT, respectively. Photomicrographs were taken on samples microtomed from compression-molded films.

Table 2. Experimental Mechanical Property Data for Nanocomposites Formed from HMW Nylon-6 and the Organoclays M_4 , $M_3(HT)_1$, and $M_2(HT)_2$

HMW nylon-6 nanocomposite		modulus (GPa)	yield strength (MPa)	elongation at break (%)	
organoclay	wt % MMT			crosshead head speed 0.51 cm/min	crosshead head speed 5.1 cm/min
	0	2.75	69.7	304	129
M_4	2.7	3.49	79.5	170	21
M_4	3.8	3.70	78.5	63	17
$M_3(HT)_1$	2.9	4.23	85.2	153	31
$M_3(HT)_1$	4.3	4.54	90.9	NA	23
$M_3(HT)_1$	4.6	4.71	90.7	10	16
$M_2(HT)_2$	3.0	3.82	84.5	174	42
$M_2(HT)_2$	4.5	4.32	87.7	60	28

Table 2 lists the mechanical properties of the three types of nanocomposites. Since the data in this table do not allow structural comparisons at fixed levels of MMT, mechanical property values were extrapolated

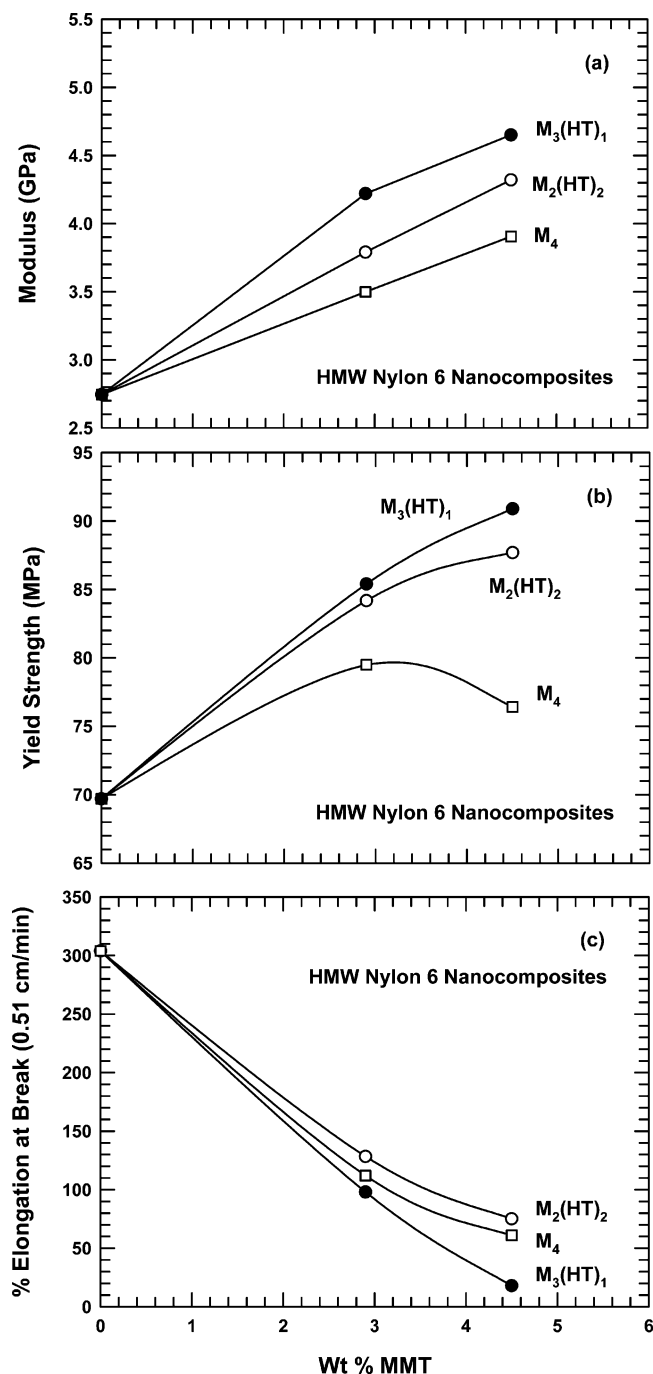


Figure 4. Effect of MMT concentration and the number of alkyl tails on the ammonium cation of the organoclay on the (a) modulus, (b) yield strength, and (c) elongation at break of nanocomposites based on HMW nylon-6.

and/or interpolated to two target loadings, 2.9 and 4.5 wt % MMT; details of the extrapolation/interpolation techniques are described in a prior publication.¹ Figure 4a shows the effect of MMT concentration on the modulus of nanocomposites formed from HMW nylon-6 and the organoclays M_4 , $M_3(HT)_1$, and $M_2(HT)_2$; note that comparisons are made on the basis of MMT content rather than on the amount of organoclay, since silicate is the reinforcing component. The nanocomposites formed from the one-tail organoclay, $M_3(HT)_1$, which consist of a well-exfoliated morphology, exhibit the highest level of stiffness enhancement, whereas those based on M_4 organoclay having no alkyl tails exhibit the least. The order in which the three curves lie agrees with the

morphological results mentioned above, which is to be expected since greater levels of organoclay exfoliation lead to higher aspect ratio filler particles which translate into better reinforcement. Similar behavior is observed in the yield strength of these materials, as seen in Figure 4b. Elongation at break data, presented in Figure 4c, shows that the more exfoliated $M_3(HT)_1$ nanocomposite is less ductile than the nanocomposites based on M_4 and $M_2(HT)_2$; generally, an increase in stiffness is often accompanied by a sacrifice in ductility.

Discussion

The above results may be explained by the effect the ammonium modifier has on the different interactions involved. Incorporation of the modifier inside the galleries of the clay by ion exchange causes the platelets to move apart. Furthermore, the size of the organic modifier will dictate the amount of gallery spacing; i.e., the larger the organic species, the greater the separation of platelets. A consequence of increasing the gallery spacing is a reduction in the level of platelet-platelet attraction up to a point; this tends to make it easier for the platelets to exfoliate. On the other hand, increasing the amount of the organic modifier seems to decrease the level of attraction between the polyamide and the organoclay, since the polyamide chains have no affinity for the aliphatic tails of the organic modifier. One would intuitively expect a repulsive interaction, or an endothermic heat of mixing, between polyamides and aliphatic units. From the work of Ellis^{14,15} the interaction energy density can be estimated to be +4.4 cal/cm³, which reflects a strongly repulsive interaction. With this in mind and the fact that organoclays can be readily exfoliated in nylon-6 and other polyamides, it follows that the polyamide chains must have an attractive energetic interaction with the pristine surface of the silicate. In fact, this notion is supported by the theoretical work of Tanaka and Goettler¹⁶ and Fermeglia et al.¹⁷ on predicting the binding energy between polyamides and quaternary alkylammonium-modified montmorillonites. By employing molecular modeling techniques, Tanaka and Goettler¹⁶ determined the highest binding energies between nylon-6,6 and the surface of montmorillonite occur for quaternary alkylammonium cations that occupy the least amount of volume. The same conclusion was arrived at by Fermeglia et al.¹⁷ when applying Tanaka and Goettler's model to predict binding energies between nylon-6 and organically modified montmorillonite.

The net favorable interaction with an organoclay that permits exfoliation in nylon-6 by melt processing results from a balance of component interactions. First, a sufficient level of platelet separation must be achieved to reduce platelet-platelet attraction. Second, it is proposed here that the polyamide-silicate contacts are much more favorable than the alkyl-silicate contacts (present in the pristine organoclay) they replace. Furthermore, this exchange of silicate contacts from alkyl to polyamide units must be sufficiently favorable to overcome the strongly unfavorable mixing of polar polyamide units with the alkyl tails of the organic modifier. Increasing the number of alkyl tails has two unfavorable effects: first, it limits the number of polyamide-silicate contacts by sterically blocking the surface, and second, it increases the amount of alkyl material that would have to mix with the polyamide.

Figure 5 schematically illustrates some of the effects of ammonium cations having zero, one, and two alkyl

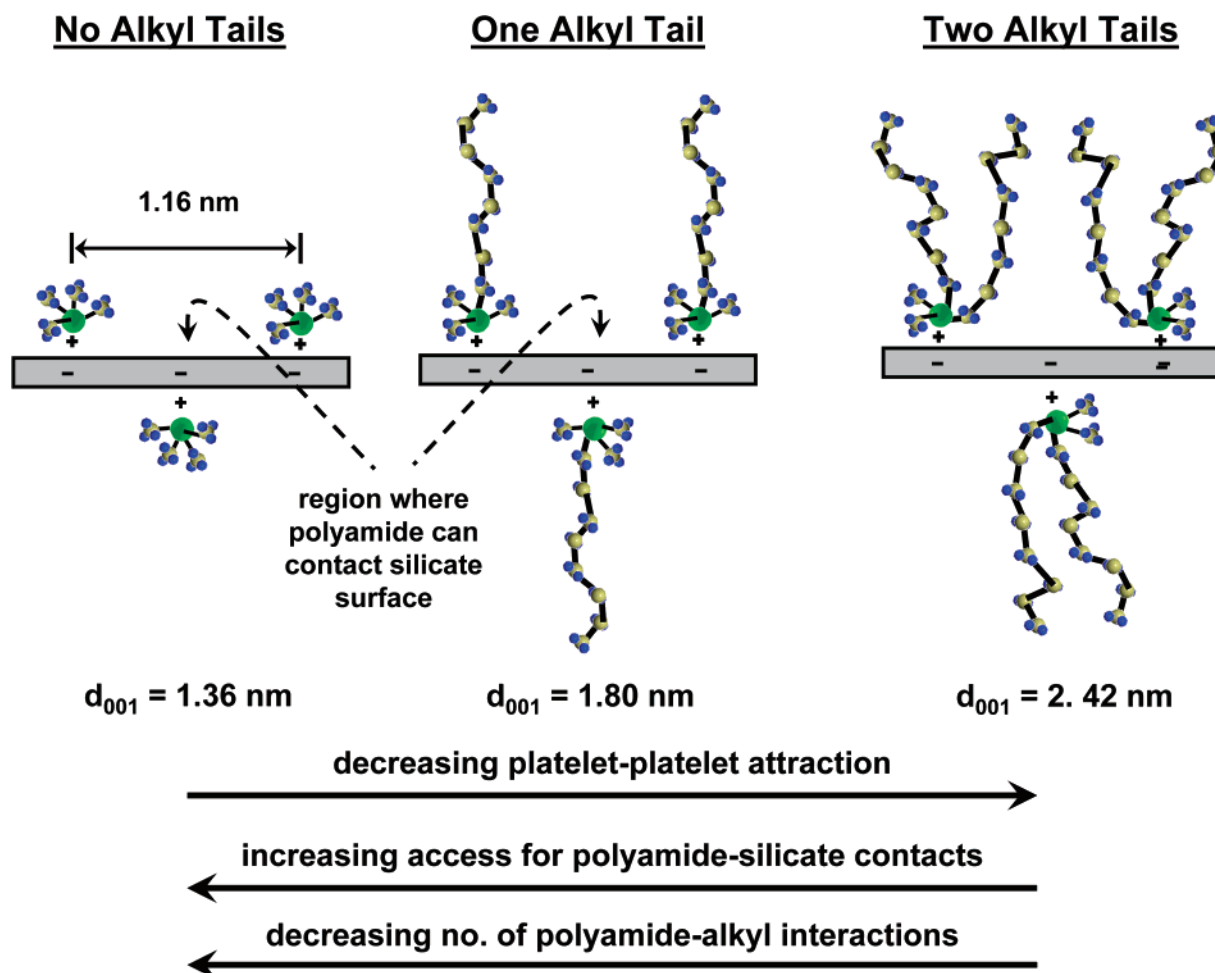


Figure 5. Illustration of the role of quaternary ammonium cations on the intercalation and exfoliation of organoclay by nylon-6.

tails have on the interaction of organoclay with nylon-6 with regard to the aforementioned component interactions. Before discussing these effects, it is important to first comment on the average distance between exchange sites and the relative size of the organic cations. The average distance between sites in these organoclays is calculated to be 1.16 nm for a clay with a cation exchange capacity of 92 mequiv/100 g of clay and a surface area of 750 m²/g; this calculation assumes that the cations are evenly distributed in a cubic array over the face of the platelet and that half of the cations are located on the one side of the clay platelet and the other half reside on the other side. The surface area of 750 m²/g is based on the value reported by van Olphen for sodium montmorillonite.¹³ Since the diameter of an alkyl unit is of the order of 0.4–0.5 nm, the spacing of 1.16 nm allows some space for the polyamide chains to access the silicate surface for a typical organic modifier; the extent to which this occurs will depend on the number and size of substituents attached to the nitrogen. Modifiers containing more than one large alkyl may, to a certain degree, sterically limit the access of the polyamide to the silicate surface.

Figure 5 shows that the organic modifier having no alkyl tails, i.e., M₄, provides the most access to the silicate surface; however, it contributes the least reduction of cohesive forces between adjacent platelets due to the small organoclay basal spacing. The lack of exfoliation observed in the corresponding M₄–nylon-6 nanocomposite strongly suggests that some level of platelet–platelet separation is essential. At the other

extreme, two alkyl tails move the platelets much farther apart, thereby greatly reducing the cohesive forces between platelets; however, at the same time, these alkyls sterically diminish the opportunity for the polymer to interact with silicate surface and increase the amount of hydrocarbon that must unfavorably mix with the polymer in order for polymer–silicate contacts to be possible. The results show that this extreme leads to a nanocomposite structure having a low level of platelet exfoliation. On the other hand, the one-tail organic modifier, M₁(HT)₃, which leads to nearly complete organoclay exfoliation in nylon-6, apparently provides a good balance between platelet spacing, level of access to exposed silicate surface, and number of unfavorable interactions between the polymer and the alkyl units. In this case, the driving force for the polyamide to contact to the silicate surface is sufficiently greater than the penalty incurred by the mixing of polyamide chains and the alkyl units of the one-tail organic modifier.

This reasoning is consistent with the views proposed by Vaia and Giannelis^{18,19} in their thermodynamic model for describing melt intercalation. They conclude that the intercalation of alkylammonium modified silicates by relatively polar polymers, like nylon-6, is facilitated by maximizing the number of favorable interactions between the polymer and the clay surface while minimizing the number of nonfavorable interactions between the polymer and the nonpolar alkylammonium cations. The one-tail organoclay provides a good balance these opposing effects.

Conclusions

The role of alkyl tails on the exfoliation of alkyl-ammonium-modified montmorillonite in nylon-6 was examined by comparing organic modifiers having zero, one, and two alkyl groups. High levels of exfoliation of these organoclays are largely governed by a balance between the amount of platelet-platelet separation, the level of exposed silicate surface that the organic modifier permits, and the number of unfavorable interactions that can occur between the aliphatic modifier and the polar polyamide. Modification of montmorillonite decreases the level of attraction between adjacent platelets by increasing the gallery spacing, yet it decreases the affinity between the nylon-6 and clay, since the interaction between hydrocarbons and polyamides is strongly repulsive. Of the three modifiers examined, the one alkyl tail modifier seems to provide an optimum combination of these effects, since a high level of exfoliation is achieved for nylon-6.

Acknowledgment. This work was supported by the Air Force Office of Scientific Research. We thank Mr. Randy Chapman of Southern Clay products for assistance with WAXS measurements and Mr. Urko Gurmendi Lostao of the University of the Basque Country for his help with various extrusion and mechanical property experiments.

References and Notes

- (1) Fornes, T. D.; Yoon, P. J.; Hunter, D. L.; Keskkula, H.; Paul, D. R. *Polymer* **2002**, *43*, 5915–5933.
- (2) Varlot, K.; Reynaud, E.; Kloppfer, M. H.; Vigier, G.; Varlet, J. J. *Polym. Sci., Part B: Polym. Phys.* **2001**, *39*, 1360–1370.
- (3) Dennis, H. R.; Hunter, D. L.; Chang, D.; Kim, S.; White, J. L.; Cho, J. W.; Paul, D. R. *Polymer* **2001**, *42*, 9513–9522.
- (4) Reichert, P.; Nitz, H.; Klinke, S.; Brandsch, R.; Thomann, R.; Mulhaupt, R. *Macromol. Mater. Eng.* **2000**, *8*–17.
- (5) Okada, A.; Usuki, A. *Mater. Sci. Eng.* **1995**, *C3*, 109–115.
- (6) Lan, T.; Kaviratna, P. D.; Pinnavaia, T. J. *Chem. Mater.* **1995**, *7*, 2144–2150.
- (7) Goettler, L. A.; Lysek, B. A.; Powell, C. E. PCT International Application, Solutia Inc., WO 9941299, 1999.
- (8) Fornes, T. D.; Yoon, P. J.; Paul, D. R. *Polymer* **2003**, *44*, 7545–7556.
- (9) Personal communication with Akzo-Nobel.
- (10) Fornes, T. D.; Yoon, P. J.; Keskkula, H.; Paul, D. R. *Polymer* **2001**, *42*, 9929–9940.
- (11) Fornes, T. D.; Yoon, P. J.; Keskkula, H.; Paul, D. R. *Polymer* **2002**, *43*, 2121–2122.
- (12) Hunter, D. L.; Knudsen, B. Personal communication.
- (13) Van Olphen, H. *An Introduction to Clay Colloid Chemistry: For Clay Technologists, Geologists, and Soil Scientists*; Wiley: New York, 1977.
- (14) Ellis, T. S. *Macromolecules* **1990**, *31*, 1058–1063.
- (15) Ellis, T. S. *Polym. Eng. Sci.* **1990**, *30*, 998–1004.
- (16) Tanaka, G.; Goettler, L. A. *Polymer* **2002**, *43*, 541–553.
- (17) Fermeglia, M.; Ferrone, M.; Pricl, S. *Fluid Phase Equilib.* **2003**, *212*, 315–329.
- (18) Vaia, R. A.; Giannelis, E. P. *Macromolecules* **1997**, *30*, 7990–7999.
- (19) Vaia, R. A.; Giannelis, E. P. *Macromolecules* **1997**, *30*, 8000–8009.

MA0305481